

Modeling of Ultra-low Energy Ion Implantation by Monte-Carlo Method

Y. Ban^{*}, S. Yoon, O. Kwon and T. Won^{**}

Division of Electrical and Computer Engineering, Inha University

253 Yonghyun-dong, Nam-gu, Inchon, Korea 402-751

^{*}ycban@hsel.emde.inha.ac.kr, ^{**}twon@hsel.emde.inha.ac.kr

ABSTRACT

In this paper, a new method for an accurate and time efficient 3D simulation of ion implantation and an ultra-low energy (sub 2keV) Monte-Carlo ion implantation model are suggested. The dopant and damage profiles show very good agreement with SIMS and RBS data, respectively. The Ion Distribution Replica Method has been implemented into the model to get a computational efficient in a 3D simulation, and we have calculated the 3D Monte-Carlo simulation into the topographically complex structure.

Keywords: low energy ion implantation, Monte-Carlo, simulation, modeling.

INTRODUCTION

The current trend of aggressive scaling of metal-oxide-semiconductor (MOS) device feature sizes down to the sub-micrometer regime has given rise to a need to form ultra-shallow junctions accurately and controllably. Low energy ion implantation therefore has the potential to play an important role in the formation of ultra-shallow junctions. The need for predictive TCAD in the area of ion implantation modeling is placing increased emphasis on accurate physical modeling of the implant process. This is particularly true for ultra-low energy implants, where dopant profiling is extremely difficult and time consuming. Using physically based model is much more efficient (once the model has been validated), since only a relatively small number of implants and measurements need to be performed.

Monte-Carlo methods based on the BCA (Binary Collision Approximation) have been used in the past for this purpose. However, a number of authors have reported on the shortcomings of the BCA at ultra-low energies [1], and it was widely believed that accurate simulation in the few keV energy range was impossible with the BCA. Molecular Dynamics (MD) has been suggested as a viable alternative [2]. However, the long computation times required for MD simulations have prompted the development of the much faster modified BCA models, suitable for low energy simulation [3].

Furthermore, since the three-dimensional computation is not tolerable without better models, it is quite requisite to develop a new simulation method with a better algorithm. In this paper, we report a three-dimensional Monte-Carlo

ion implantation model based on BCA energies. The dopant and damage profiles show very good agreement with SIMS (Secondary Ion Mass Spectroscopy) data and RBS (Rutherford Backscattering Spectroscopy) data, respectively. Moreover, the Ion Distribution Replica Method has been implemented into the model to get a computational efficient in a 3D simulation, and we have calculated the 3D Monte-Carlo simulation into the topographically complex structure. This work reports on the integration of the implantation code into the 3D topography simulator 3D-SURFILER (SUFface proFILER) [4] as an optional model.

SIMULATION MODELS

An ion traveling through a silicon crystal experiences repulsive electric fields from several sources. The first comes from the screened coulomb electric field of the nucleus of the silicon atoms. This give rise to the nuclear stopping. The second source of stopping mechanism is the effect of polarization of electrons on the electric field, this give rise to non-local electronic stopping. The third stopping force comes from the interaction of the electronic cloud of the ion with the more tightly bound electrons of the Si target atoms. The electrons can transfer a part of their momentum to the electrons of the targets, thereby causing a reduction of the overall energy of the ion; this give rise to local electronic stopping.

There are two part of electronic stopping that need to be taken into account: the electronic loss between collision and the electronic loss during collision. First, the following expression is used to obtain the inelastic electronics loss between collisions [5]:

$$\frac{dE}{dx} = \frac{4\pi q^4 \rho}{\epsilon_0^2 m v^2} L, \quad (1)$$

where v and m are the velocity and mass of ion in the silicon respectively, and ρ is the electron density at the position of the ion.

The physical model for local electronic stopping is based on the Firsov [6] and Morris [5] models. Firsov's theory assumes that energy transfer from the electrons of the ion to the electrons of the target occurs by transfer of electrons between the two atoms.

The orbital velocity of the electrons v is assumed to be much higher than their average velocity, which is just the velocity of the ion. The target is assumed to be at rest. Then, an electron transferred from the ion to the target will also transfer momentum $m_e(v_{target} - v_{ion})$ to the target, where v_{ion} and v_{target} are the average velocity of the ion and target electrons, respectively. The electron current density from ion to target will be proportional to the local electron concentration multiplied by the orbital velocity (rather than the total electron velocity, since the ion velocity can be neglected). Thus, the total force exerted by the target on the ion can be written as in Eq. (2).

$$\dot{F} = m_e(\dot{V}_{target} - \dot{V}_{ion}) \cdot \frac{nv}{4} dS, \quad (2)$$

where v is the electron orbital velocity, and the integration is across the plane bisecting the relative position vector of the ion and target.

The goal of the improved multi-body collision algorithm is to simulate multi-body collisions within the paradigm of the BCA. This is accomplished through the use of modified inter-atomic pair-potentials which simulate the effect of three-body potentials. If we assume that the total inter-atomic potential acting on the ion is simply a linear superposition of the pair potentials arising from the interaction with individual silicon target atoms (i.e. the silicon atoms do not act on one another), we can see that the force acting on the ion in the region where the potentials overlap will be considerably weaker than if the potentials acted individually, with the force actually vanishing at the halfway point between silicon atoms. For the sake of computational tractability, the model is confined to three-body interactions only (i.e. the ion and up to two silicon atoms).

In this work, if E_1 and E_2 are the value of nuclear stopping associated with the 2-body and 3-body calculations, the final value for the nuclear stopping E is obtained from Eq. (3).

$$E = \frac{E_1}{\exp \frac{-b-b_0}{0.1} \sqrt{+1}} + \frac{E_2}{\exp \frac{-b_0-b}{0.1} \sqrt{+1}} \quad (3)$$

The impact parameter of the collision is denoted with b , while b_0 is the impact parameter at which the weights for both the 2 and 3-body collisions are.

To achieve the same statistical accuracy of three-dimensional simulations as in two-dimension, the number of ions traced should be considerably increased. Therefore, the CPU time grows approximately proportional to the surface area of the simulation domain [7]. The fundamental idea to reduce the simulation time leads to the development

of the Ion Distribution Replica Method as shown in Fig. 1. The idea is to generate a relatively small number of model trajectories, and re-use them wherever possible throughout the topography.

The new algorithm is justified by the superposition law: <1> subdivide the width of the simulation area into sub-windows; <2> calculate physical trajectories in a target; <3> make copies of this trajectory if the simulation environments coincide with that of the precedence (\sim in Fig. 1); <4> follow each trajectory copy and recalculate an ion trajectory if a new simulation environment is detected (\sim in Fig. 1).

SIMULATION RESULTS

Fig. 2 shows the comparison of the simulation results (solid line) with SIMS experimental data [8,9] for boron implants at varying energies. The dose are $1 \times 10^{12} \text{ cm}^{-2}$ for the 500eV implant, $3 \times 10^{13} \text{ cm}^{-2}$ for the 1keV and 2keV implants. Since low energy profiles are extremely shallow, they are critically dependent on the thickness of the surface oxide. Thus, it is necessary to control the oxide thickness accurately for the purpose of model validation. Therefore, the oxide thickness values used range from 0.5nm for $2 \times 10^{12} \text{ cm}^{-2}$ dose, to 2.0nm for 10^{15} cm^{-2} dose. A thin amorphous layer (0.5nm) on the surface was used to simulate the surface roughness of the wafer surface. As shown in Fig. 3, very good agreement between SIMS profiles [9] and simulation results was observed for the low energy ion implantation profiles.

Fig. 3 shows the comparison of the simulation results with SIMS profiles [9] for 2keV arsenic implants at a dose of $6 \times 10^{12} \text{ cm}^{-2}$, for on-axis and off-axis implants. It can be seen that the impurity profiles ate in very good agreement with the SIMS impurity profiles, the channeling tail drop very steeply with depth. This phenomenon is due to the large atomic mass of arsenic.

Fig. 4 shows the comparison of the simulation results with SIMS profiles [9] for 2keV boron implants as a function of dose. The simulated oxide thickness is allowed to vary with dose i.e. 0.5nm for 10^{13} cm^{-2} and $3 \times 10^{13} \text{ cm}^{-2}$ doses, 0.8nm for 10^{14} cm^{-2} dose, 1.2nm for $3 \times 10^{14} \text{ cm}^{-2}$ dose and 1.7nm for 10^{15} cm^{-2} dose. As shown in Fig. 4, excellent agreement has been obtained between the simulations and experiments.

Fig. 5 shows the comparison of the simulation results with RBS profiles [10] for both arsenic implant at energy of 50keV and a dose of $1 \times 10^{14} \text{ cm}^{-2}$ and BF2 implant at energy of 65keV and a dose of $5 \times 10^{14} \text{ cm}^{-2}$. The flat tails of the experimental data are due to RBS background noise, and hence should be ignored. The 100% defect concentration for previously defined N_α had been set to be 10% of silicon density for all implant species.

Fig. 6 shows the 3D boron profile for 10keV implantation into (100) Si, into the [100] channel direction, for dose $5 \times 10^{14} \text{ cm}^{-2}$. The window area of the implanted

region is $2,000 \times 2,000$, and the total number of boron and pseudo-projectiles followed in the simulations is 1,200,000 for each dose. In the figure, the color scale and the level of contour lines denote the common logarithm of the concentration (cm^{-3}) divided by the dose (cm^{-2}). This results in an insufficient number of events at low concentration areas and leads to statistical noise that cannot be tolerated. For that reason, we have implemented the trajectory split method [11,12] for the Monte-Carlo simulation of ion implantation to reduce the computational effort of three-dimensional simulation. The 3D profile in Fig. 6 shows that at least two orders of magnitude below the maximum concentration, lateral channeling is present. The corner rounding effect can also be seen in the 3D figure. The estimated simulation time is 73 minutes in SUN ultra-10 workstation. In the meanwhile, the estimated time without Ion Distribution Replica Method for the same problem is over 1 day.

Fig. 7 provides an example of the application of the cell-based algorithm [4] to $0.1\mu\text{m}$ MOSFET structure. Different materials are denoted with different colors, with blue region corresponding to silicon substrate, gray to STI and silicon dioxide, yellow to nitride sidewall spacer, and red to poly-silicon gate. A 3D dopant distribution in Fig. 8 is formed by a zero degree tilted 10keV arsenic implantation with a dose of $5 \cdot 10^{15}/\text{cm}^2$ to $0.1\mu\text{m}$ MOSFET structure as shown in Fig. 7. Estimated CPU time is 97 minutes in SUN ultra-10 workstation and the Ion Distribution Replica Method for the topographically complex structure reduces the simulation time by a few orders of magnitude, with no loss of accuracy for the three-dimensional Monte Carlo ion implantation simulation.

CONCLUSIONS

A Monte-Carlo simulator of ion implantation has been successfully integrated into the 3D process simulator 3D-SURFILER. The data exchange between the implantation module and the 3D-SURFILER environment is very efficient and it is organized in such a manner that the implantation module is ready for use in a future 3D simulator. Furthermore, our implantation simulator is capable of modeling implants into arbitrary three-dimensional topography with various materials and initial doping concentration.

Our simulator has implemented the ultra-low energy (sub 2keV) ion implantation module for predicting doping profiles and damage profiles. It has been shown that the impurity profiles and the damage profiles are in very good agreement with the SIMS profiles and the RBS profiles, respectively. Further work is in progress to integrate the next thermal process simulations such as transient enhanced diffusion (TED).

ACKNOWLEDGEMENT

This work was supported by Korean Ministry of Information and Communication and COSAR.

REFERENCES

- [1] Gartner et al., *Nucl. Instrum. Methods Phys. Res. B* **83**, pp. 87-94, 1993.
- [2] K. Beardmore, *Proceedings of IIT*, pp. 535, 1996.
- [3] Y. Ban et al., *JKPS*, vol. **35**, pp. s829-s833, 1999.
- [4] T. Won, *JKPS*, vol. **33**, pp. s72-s75, 1998.
- [5] S. Morris et al., *IEDM*, pp. 721-724, 1996.
- [6] O. Firsov, *Sov. Ph-JETP*, vol. **36**, pp. 1076-1080, 1959.
- [7] M. Posselt, *Nucl. Inst. and Meth. B*, vol. **96**, pp. 163-167, 1995.
- [8] G. Hobler et al., *IEDM*, pp. 489-492, 1997.
- [9] B. Obradovic et al., *Proc. of SPIE, Micro. Dev. Tech.*, vol. **3212**, pp. 342-353, 1998.
- [10] S. Tian, *Ph.D. Thesis, The University of Texas at Austin*, 1997.
- [11] S. Yang et al., *NUPAD V*, pp. 97-100, 1994.
- [12] W. Bohmayr et al., *IEEE Trans. Semicon. Manu.*, vol. **8**, pp. 402-407, 1995.

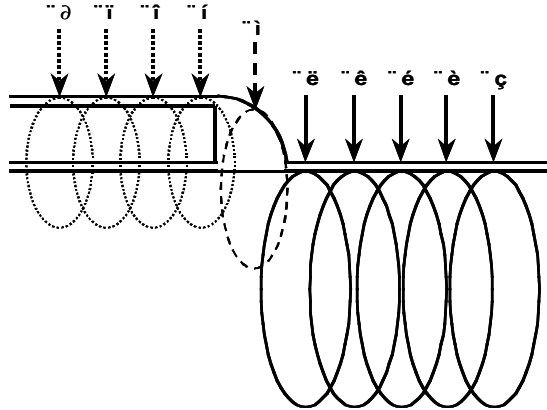


Fig. 1. A plot describing the definition of the Ion Distribution Replica Method.

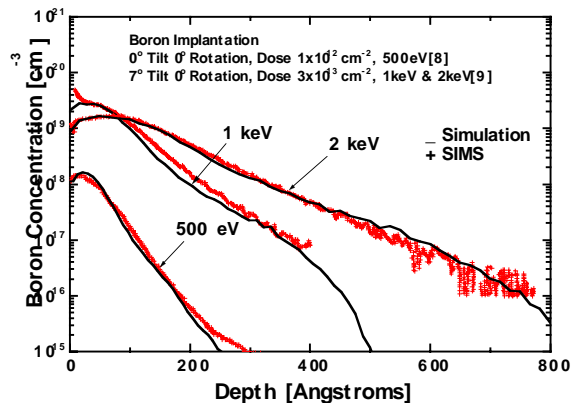


Fig. 2. A plot showing the comparison of the simulation results with SIMS [8,9] profiles for 500eV, 1keV and 2keV boron implants.

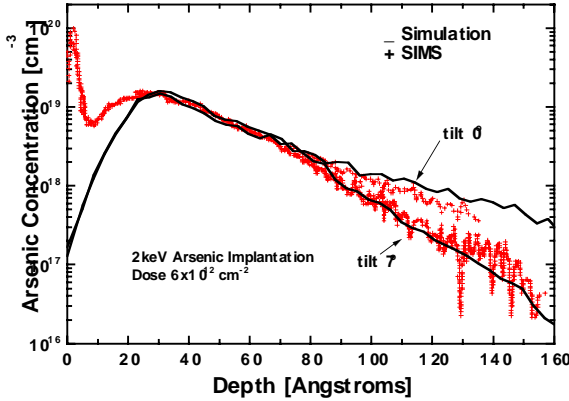


Fig. 3. A plot showing the comparison of the simulation results with SIMS [9] profiles for 2keV arsenic implants.

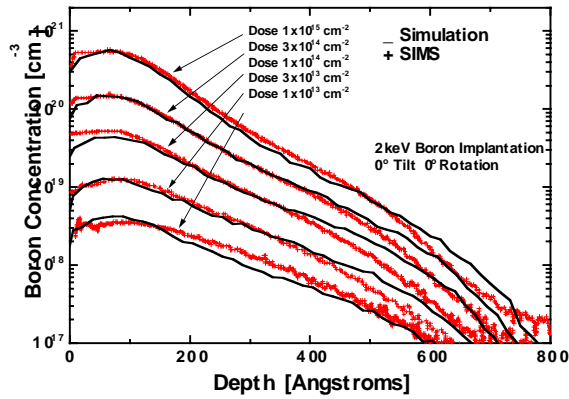


Fig. 4. A plot showing the comparison of the simulation results with SIMS [9] profiles for 2keV boron implants, at various doses.

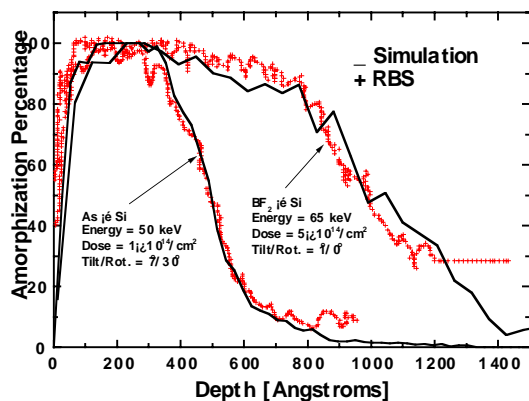


Fig. 5. A plot showing the comparison of the simulation results with RBS [10] profiles for arsenic implants.

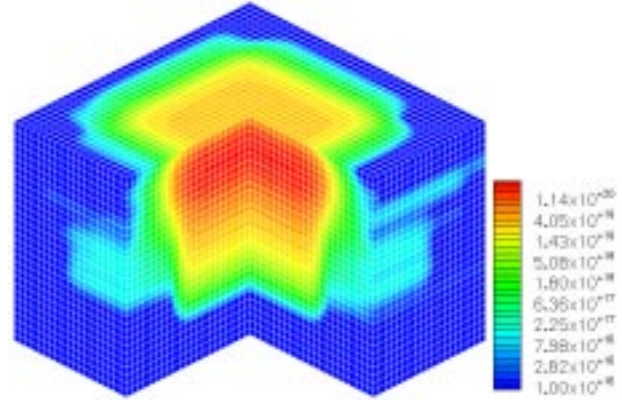


Fig. 6. Simulation results of the 3D boron concentration at energy of 10keV, dose $5 \cdot 10^{14}/\text{cm}^2$, tilt 0° , and rotation 0° . The area of the implants region is $2,000 \times 2,000 \mu\text{m}^2$.

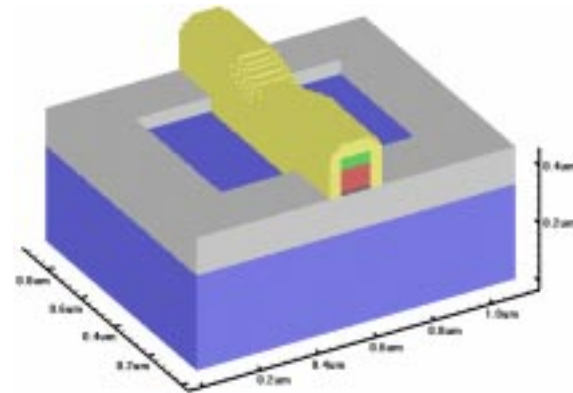


Fig. 7. A plot showing an application of the cell-based algorithm to $0.1\mu\text{m}$ MOSFET structure.

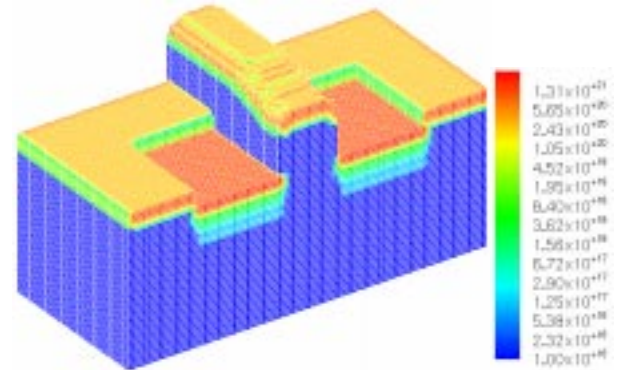


Fig. 8. A plot showing a three dimensional arsenic dopant distribution of $0.1\mu\text{m}$ NMOSFET at energy of 10keV, dose $5 \cdot 10^{15}/\text{cm}^2$, and tilt 0° .